Metallurgy and materials
Metalurgia e materiais

Evaluation of internal corrosion in a Brazilian iron ore slurry pipeline based on the characterization of scales and tubercles

http://dx.doi.org/10.1590/0370-44672017710073

Gabriela Goes Mattioli
Engenheira de Processo
Samarco Mineração S.A.
Unidade Industrial de Germano
Mariana - Minas Gerais - Brasil
gabimattioli@hotmail.com; gabriela.goes@samarco.com

Afonso Henriques Martins
Professor-Titular
Universidade Federal de Minas Gerais – UFMG
Escola de Engenharia
Departamento de Engenharia Metalúrgica e Materiais
Belo Horizonte – Minas Gerais - Brasil
ahmartin@demet.ufmg.br

Vanessa de Freitas Cunha Lins
Professor-Titular
Universidade Federal de Minas Gerais – UFMG
Escola de Engenharia
Departamento de Engenharia Química
Belo Horizonte – Minas Gerais - Brasil
vlins@deq.ufmg.br

Paulo Roberto Gomes Brandão
Professor Emérito
Universidade Federal de Minas Gerais – UFMG
Escola de Engenharia
Departamento de Engenharia de Minas
Belo Horizonte – Minas Gerais - Brasil
pbrandao@demin.ufmg.br

Ayron Silva Guimarães Torres
Engenheiro de Integridade
Samarco Mineração S.A.
Unidade Industrial de Germano
Mariana - Minas Gerais - Brasil
ayront@gmail.com; ayron.torres@samarco.com

Abstract

The transport capacity of long-distance slurry pumping systems is directly related to the roughness of the pipe. In this context, corrosion plays an important role, especially when dealing with old pipes. Chemical, mineralogical and microstructural analyses were performed on materials removed from the internal surface of an iron ore slurry pipeline in order to access their composition and to check if they were a result of internal pipeline corrosion. This pipeline has been operating since 1977. It was found that the tubercles formed on the internal wall of the pipe presented botryoidal magnetite as their essential composition. As the amount of magnetite is very low in the transported slurry and magnetite with botryoidal morphology is not present in the processed iron ore, it was concluded that this magnetite is a result of a corrosion process occurring on the internal wall of the pipeline.

Keywords: internal corrosion, slurry pipeline, tubercle, botryoidal magnetite.

1. Introduction

The transport of iron ore slurry through pipelines has several advantages over other modes of transport on long distances, such as lower rate of accidents during operation, lower power consumption, higher reliability, savings in transport costs and relatively low environmental impact (Sampaio; Brandão, 2004).

The transport capacity of slurry pipelines is directly related to the roughness of the pipe. In this context, corrosion plays an important role, especially when dealing with old pipes such as the studied pipeline which has been in operation since 1977, transporting iron ore slurry from the beneficiation process to the filtering and the pelletizing processes and, therefore, subjected to corrosive processes that alter its surface roughness. An intense tubercle formation is observed on the internal wall of the pipes, especially in kilometers near the pumping stations. In order to access the composition of these tubercles and to check if they were, in fact, a result of internal pipeline corrosion, this work of characterizing the corrosion scales and tubercles removed from the pipe was conducted. The pipeline was made of carbon steel without inner lining and meets the requirements of the API 5L X60 standard.

According to WOLYNEC (2003), corrosion in aqueous media represents 90 % of metal corrosion failures. Among the sectors most seriously affected by corrosion, SILVA (1981) cites the mining, specifically because of the corrosive processes that affect iron ore slurry pipelines and their equipment.

2. Materials and methods

Samples of pipe scales and tubercles removed by pig were analyzed in order to access their chemical and mineralogical compositions. A pig is a tool used for cleaning and/or for inspecting the internal surfaces of pipelines. After being inserted into the pipe, the pig travels through it, driven by the flow being pumped.

The overall sample had a grain size between 3.35 mm and 0.15 mm. The chemical analysis was made by the wet method through the dichromatometry technique for Fe_2O_3 and FeO; CaO, SiO_2, Al_2O_3, P and MnO_2 were analyzed by atomic emission spectroscopy with inductive coupled plasma (ICPAES). The atomic emission spectrometer used was Ciros, CCD model. Iron contents were converted from Fe to Fe_2O_3. Loss on ignition (LOI) was determined by calcination in an oven and the consequent weight difference. Polished sections were prepared for microscopic studies. Only diamond pastes were used in the polishing step with loose abrasives. Samples were pulverized in a pot mill and were analyzed by X-ray diffraction and X-ray fluorescence spectrometry. The X-ray diffractometer used was Philips (Panalytical) for powder samples, with an X'Pert-APD system, PW 3710/31 controller. The X-ray fluorescence spectrometer used was Philips (Panalytical), PW 2400 model. The microstructural studies were carried out by scanning electron microscopy (SEM) with micro-analysis done by energy-dispersive X-ray spectrometry (EDS). The SEM used was the FEI, Inspect S50 model and the EDS was the Edax, Genesis model. Backscattered electron images were used. A very thin film of gold was deposited on the polished samples to promote surface electrical conduction. CO_2 concentrations shown were calculated from the stoichiometry of calcite ($CaCO_3$) from trusted levels of CaO when the carbon characteristic peak was clear.

3. Results

A sample of the granular materials removed by the pig from the internal surface of the pipeline containing tubercles and corrosion scales was analyzed and the obtained results are presented in Table 1. Table 2 shows the sample mineralogical composition. The data are mainly from X-ray diffraction, complemented by chemical analysis and studies by SEM with EDS micro-analysis.

Fe_2O_3	FeO	CaO	PPC	SiO_2	Al_2O_3	P	MnO_2	Total
80.56	7.14	2.91	5.59	2.25	0.58	0.082	0.84	99.95

Table 1
Sample chemical composition (wt %).

Magnetite	Hematite	Quartz	Goethite	Calcite
23.0	40.7	2.3	28.8	5.2

Table 2
Sample mineralogical composition (wt %).

It is noteworthy that the analyzed tubercles exhibit a ferromagnetic property, being drawn when a magnet was approximated.

The results of semi-quantitative chemical analysis performed by X-ray fluorescence spectrometry of the global sample presented high iron and oxygen concentration, moderate content of silicon, calcium and carbon, low content of manganese and phosphorus and traces of aluminum, sulfur and chromium.

Figure 1 shows a typical tubercle image, obtained using SEM with backscattered electrons.

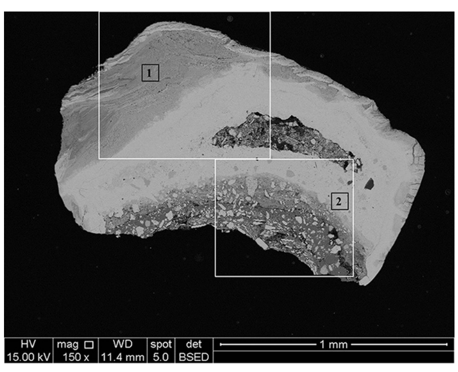

Figure 1
Typical tubercle (polished section).

From the analysis of this tubercle it was found that it is a particle mainly composed of botryoidal magnetite (light grey) which presents thin, parallel and concentric (when curved) layers, bright and dark, with radial arrangement of crystallites. On the bottom of the tubercle and inside it there are darker layers with bonded aggregates. The details of Figure 1 identified as regions 1 and 2 are shown in Figure 2 and in Figure 3, respectively, which were also obtained using SEM with backscattered electrons.

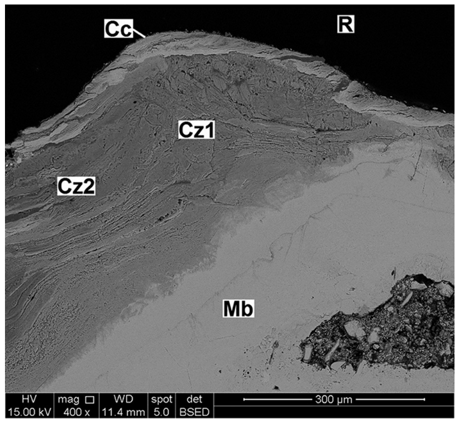

Figure 2
Detail 1 of Figure 1,
emphasizing the upper region of the tubercle.

In Figure 2, it is possible to observe a darker layer (Cz) above and on the left of the main botryoidal magnetite (Mb) region. The lighter scale observed is tagged as Cc. On the bottom right, there is a pore filled by an aggregate of very small particles. The region marked as R consists only of the impregnation resin. Microanalyses of the various features are shown in Table 3. From these results, it may be considered that the four areas flagged in Figure 2 basically comprise botryoidal magnetite.

Table 3
Microanalyses of the
areas shown in Figure 2.

Area	SiO_2	Al_2O_3	Fe_2O_3	MgO	CaO	Na_2O	MnO	SO_3	P_2O_5	CO_2	Mineral or phase
Mb	0.0	0.0	99.3	0.0	0.0	0.0	0.7	0.0	0.0	0.0	Botryoidal magnetite
Cz1	1.3	1.4	91.4	0.0	2.6	0.0	1.3	0.0	0.0	2.0	Botryoidal magnetite with low Ca, Al, Si
Cz2	1.3	1.4	88.0	0.5	2.5	0.5	1.2	1.2	1.4	2.0	Botryoidal magnetite with Ca, Al, Si and other elements
Cc	1.3	0.5	93.4	0.0	1.6	0.0	1.9	0.0	0.0	1.3	Botryoidal magnetite with low Ca, Al, Si

In Figure 3, layers of gray tones (Cz1 and Cz2) and aggregates of small particles of lamellar hematite immersed in the gray layer (Ag1) are visible. Above, amid the botryoidal magnetite region, there are darker spots (Mce). Microanalyses of the various features are shown in Table 4.

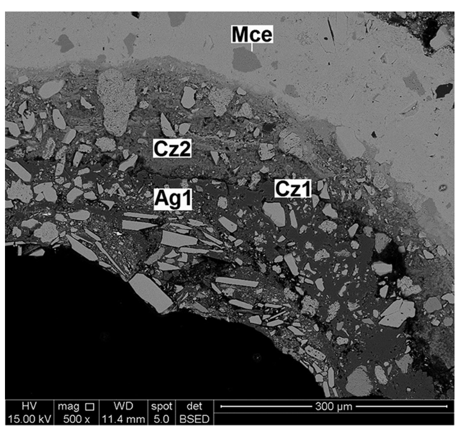

Figure 3
Detail 2 of Figure 1, emphasizing
the lower region of the tubercle.

Area	SiO_2	Al_2O_3	Fe_2O_3	CaO	MnO	CO_2	Mineral or phase
Mce	3.4	0.0	96.1	0.0	0.5	0.0	Botryoidal magnetite with Si
Cz1	0.0	0.0	2.6	54.6	0.0	42.8	Calcite
Cz2	1.7	2.7	90.8	1.5	2.1	1.2	Goethite with Ca and Mn
Ag1	3.8	0.0	20.1	42.6	0.0	33.5	Calcite with iron minerals and quartz

Table 4
Microanalyses of the areas shown in Figure 3.

Another typical tubercle was identified in the sample and its image, taken with SEM with backscattered electrons, is shown in Figure 4. The analysis of this tubercle showed that it is mainly composed of botryoidal magnetite (light gray), with darker layers and with aggregates adhered to the right and to the inside. The largest and the smallest areas marked in Figure 4 are presented, respectively, in Figure 5 and Figure 6, obtained with SEM with backscattered electrons.

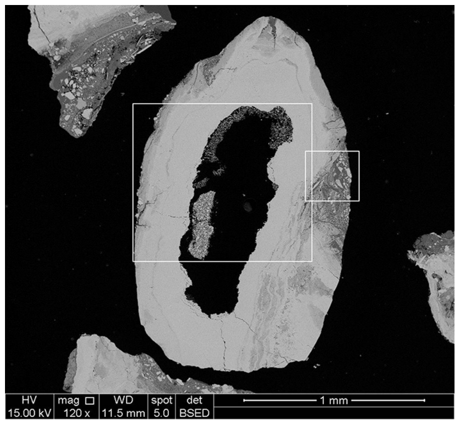

Figure 4
Another typical tubercle.

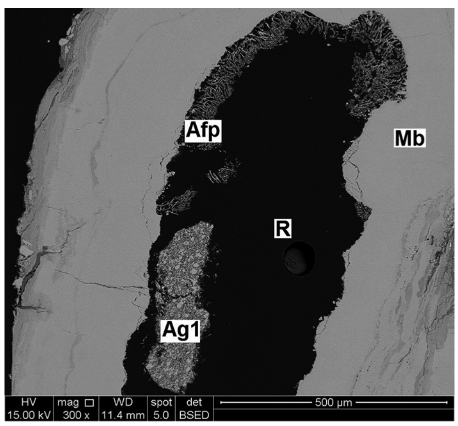

Figure 5
Detail of the largest area flagged in Figure 4.

In Figure 5, a large pore partially filled with a porous fiber aggregate (Afp) and a dense aggregate (Ag1) is observed. Thin bands with darker tones of gray are noted within the botryoidal magnetite (Mb). The dark area marked as R consists only of the impregnation resin. Microanalyses of the various features are shown in Table 5.

Area	SiO_2	Al_2O_3	Fe_2O_3	CaO	MnO	CO_2	Mineral or phase
Mb	0.0	0.0	99.2	0.0	0.8	0.0	Botryoidal magnetite
Afp	0.9	0.7	98.4	0.0	0.0	0.0	Probably fibrous goethite
Ag1	0.9	1.0	97.6	0.0	0.4	0.0	Iron minerals

Table 5
Microanalyses of the areas shown in Figure 5.

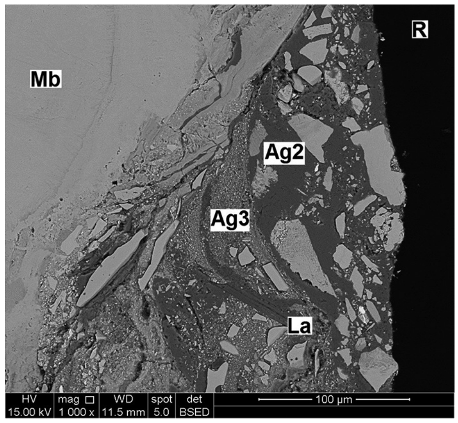

Figure 6
Detail of the smallest area marked in Figure 4.

In Figure 6, there is a complex aggregate of particles of lamellar hematite and other iron minerals; locally these particles are very small (Ag3). The cement of the aggregate is darker (Ag2) and is mainly composed of calcite. There is a lamella (La) of muscovite mica. Microanalyses of the areas marked as Ag2, Ag3 and La are shown in Table 6.

Table 6
Microanalyses of some areas highlighted in Figure 6.

Area	SiO_2	$Al2O_3$	Fe_2O_3	CaO	MgO	K_2O	Na_2O	P_2O_5	CO_2	Mineral or phase
Ag2	0.5	0.0	3.9	53.6	0.0	0.0	0.0	0.0	42.0	Calcite
Ag3	1.4	0.7	38.9	30.0	0.0	0.0	0.0	11.8	17.2	Iron minerals with calcite and phosphate
La	45.5	27.6	7.2	4.9	1.6	9.2	0.2	0.0	3.8	Muscovite mica

A fragment of a typical tubercle in the sample was analyzed. It was found that it is a particle mainly composed of botryoidal magnetite (light gray) with darker layers and scales and adhered aggregates, mainly in the upper region and within the cavity. Its image taken with SEM with backscattered electrons is shown in Figure 7.

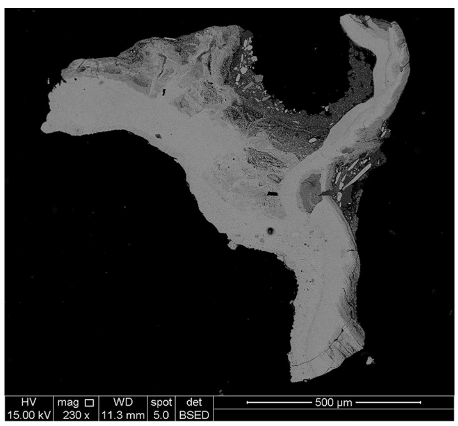

Figure 7
Fragment of a typical tubercle.

4. Discussion

HAJJ *et al.* (2013) state that the mechanism of steel corrosion depends essentially on the presence or absence of oxygen. In the presence of oxygen, aqueous corrosion is governed by the formation of different oxides and oxyhydroxides of iron (III) and, therefore, lepidocrocite, goethite, maghemite and hematite are likely to form, whereas in the absence of oxygen, more magnetite formation occurs on the metal surface.

Hematite and goethite are predominant minerals in the slurry transported through the pipeline, since it is composed of about 79 % of hematite, 18 % of goethite and 3 % of magnetite. This is explained by the fact that hematite and goethite are predominant minerals in the Alegria complex, where the company mines some pits (ROCHA, 2008). It is noteworthy that in the geological context of the Alegria deposit, magnetite does not occur with botryoidal morphology, as can be seen in the studies of ROCHA (1997, 2008) which described the morphology of Alegria's ores. Furthermore, the presence of magnetite with this morphology in the Quadrilátero Ferrífero (Iron Quadrangle region) has not been reported.

The most abundant mineral phases found in the tubercles analyzes were hematite, magnetite and goethite, with the latter two having fairly close abundance, while hematite is the majority. However, the phase that is the main cause of the ferromagnetic property of the tubercles removed from the pipeline is magnetite, with botryoidal morphology, more rarely massive. The fact that the amount of magnetite present originally in the transported slurry is very low, besides the fact that there is no geological evidence of this type of magnetite morphology in Alegria's ores, indicates that this detected magnetite is formed by the pipe's steel oxidation. The fourth phase in abundance is calcite, derived from the calcium hydroxide added to the concentrate (in the form of lime water) before pumping in order to modify its rheology and increase its pH. The aggregates that are finest and richest in calcium are formed by a mixture of calcite with fine particles of iron ore, forming a "mortar". But the essential and original structure of the tubercles does not contain significant amounts of calcium which would therefore not be associated with their formation.

Traces of potassium oxide (K_2O), magnesium oxide (MgO) and sodium oxide (Na_2O) found in the samples may be originated from ore contaminants (ROCHA, 1997). The presence of alumina (Al_2O3), phosphorus compounds and silica (SiO_2) was already expected, as these are some of the main contaminants of the ore transported, as reported by ROCHA (1997). Traces of manganese may be originated from ore (ROCHA, 1997), or even from the pipe steel. The presence of sulfur compounds may be linked to contaminants of the ore and/or of the lime, as the lime specification allows the presence of traces of this element. The detected traces of chromium may be originated from the grinding bodies used in milling.

5. Conclusions

The tubercles removed from the pipeline are composed mainly by botryoidal magnetite. This magnetite is formed by the oxidation of the pipeline steel; it should be noted that in the geological context of the Alegria complex, where the ore is mined, the magnetite does not occur with botryoidal morphology. Furthermore, the presence of magnetite with this morphology in the Quadrilátero Ferrífero (Iron Quadrangle region) has not been reported. Hematite and goethite were also identified in abundance in the tubercles. Although calcite, derived from calcium hydroxide added to the concentrate, is the fourth phase identified in abundance in the tubercles, the essential and original structure of them does not contain significant amounts of calcium, which would therefore not be associated with their formation.

References

HAJJ, H. E., ABDELOUAS, A., MENDILI Y. E., KARAKURT, G., GRAMBOW, B., MARTIN, C. Corrosion of carbon steel under sequential aerobic–anaerobic environmental conditions. ***Corrosion Science,*** v.76, p.432–440, jul. 2013.

ROCHA, J. M. P. ***Caracterização mineralógica de minérios goethíticos-limoníticos da mina de Alegria, M.G.*** Belo Horizonte: Universidade Federal de Minas Gerais, 1997. p. 77, 167-168. (Dissertação, Mestrado em Engenharia Metalúrgica e de Minas).

ROCHA, J. M. P. ***Definição da tipologia e caracterização mineralógica e microestrutural dos itabiritos anfibolíticos das minas de Alegria da Samarco Mineração S.A. – Minas Gerais.*** Belo Horizonte: Universidade Federal de Minas Gerais, 2008. v.1, p.52, 65. (Tese, Doutorado em Engenharia Metalúrgica e de Minas).

SAMPAIO, D. A., BRANDÃO, P. R. G. Rheological properties of iron ore concentrates produced by Samarco Mineração S.A. (Samarco) and their effect on the potential of plug formation of the pipeline. In: INTERNATIONAL CONFERENCE ON HYDROTRANSPORT, 16. Santiago, 2004. In: INTERNATIONAL CONFERENCE, 16. Bedfordshire: BHR Group Limited, 2004. p. 231-243. (Papers presented at Hydrotransport).

SILVA, P. F. Introdução à corrosão e proteção das superfícies metálicas. Belo Horizonte: Imprensa Universitária, UFMG, 1981. 357p.

WOLYNEC, S. ***Técnicas eletroquímicas em corrosão.*** São Paulo: EDUSP, 2003.

Received: 16 May 2017 - Accepted: 23 October 2017.